This is a preprint version of manuscript- doi: 10.1021/acs.langmuir.8b03635

Here is the link to the published article -
https://pubs.acs.org/doi/10.1021/acs.langmuir.8b03635

Using Imaging Flow Cytometry to Quantify and Optimize Giant Vesicle Production by Water-in-oil Emulsion Transfer Methods

Yuka Matsushita-Ishiodori,[†] Martin M. Hanczyc,[‡,§] Anna Wang, [∥,#] Jack W. Szostak, [∥,⊥,#] and Tetsuya Yomo[*,†]

[†]Institute of Biology and Information Science, School of Computer Science and Software Engineering, School of Life Sciences, East China Normal University, Shanghai 200062, PR China.

[‡]Laboratory for Artificial Biology, Centre for Integrative Biology (CIBIO), University of Trento, 38123, Trento, Italy.

[§]Chemical and Biological Engineering, University of New Mexico, MSC011120, Albuquerque, NM, 87131-0001, USA.

[∥]Department of Molecular Biology, Massachusetts General Hospital, Boston, Massachusetts 02114, United States

[⊥]Department of Genetics, Harvard Medical School, Boston, Massachusetts 02114, United States

[#]Center for Computational and Integrative Biology, Massachusetts General Hospital,

Boston, Massachusetts 02114, United States

KEYWORDS

Giant vesicles, POPC, water-in-oil emulsion transfer method, *imaging* flow cytometry

ABSTRACT

Many biologists, biochemists, and biophysicists study giant vesicles, which have a diameter of >1 μm, owing to their ease of characterization using standard optical methods. More recently, there has been interest in using giant vesicles as model systems for living cells and for the construction of artificial cells. In fact, there have been a number of reports about functionalizing giant vesicles using membrane-bound pore proteins and encapsulating biochemical reactions. Among the various methods for preparing giant vesicles, the water-in-oil emulsion transfer method is particularly well established. However, the giant vesicles prepared by this method have complex and heterogeneous properties, such as particle size and membrane structure. Here we demonstrate the characterization of giant vesicles by *imaging* flow cytometry to provide quantitative and qualitative information about the vesicle products prepared by the water-in-oil emulsion transfer method. Through image-based analyses, several kinds of protocol by-products, such as oil droplets and vesicles encapsulating no target molecules, were identified and successfully quantified. Further, the optimal agitation conditions for the water-in-oil emulsion transfer method were found from detailed analysis of *imaging* flow cytometry data. Our results indicate that a sonication-based water-in-oil emulsion transfer method exhibited a higher efficiency in producing giant vesicles - about 10 times or

higher than that of vortex- and rumble strip-based methods. It is anticipated that these approaches will be useful for fine-tuning giant vesicle production and subsequent applications.

GRAPHICAL ABSTRACT

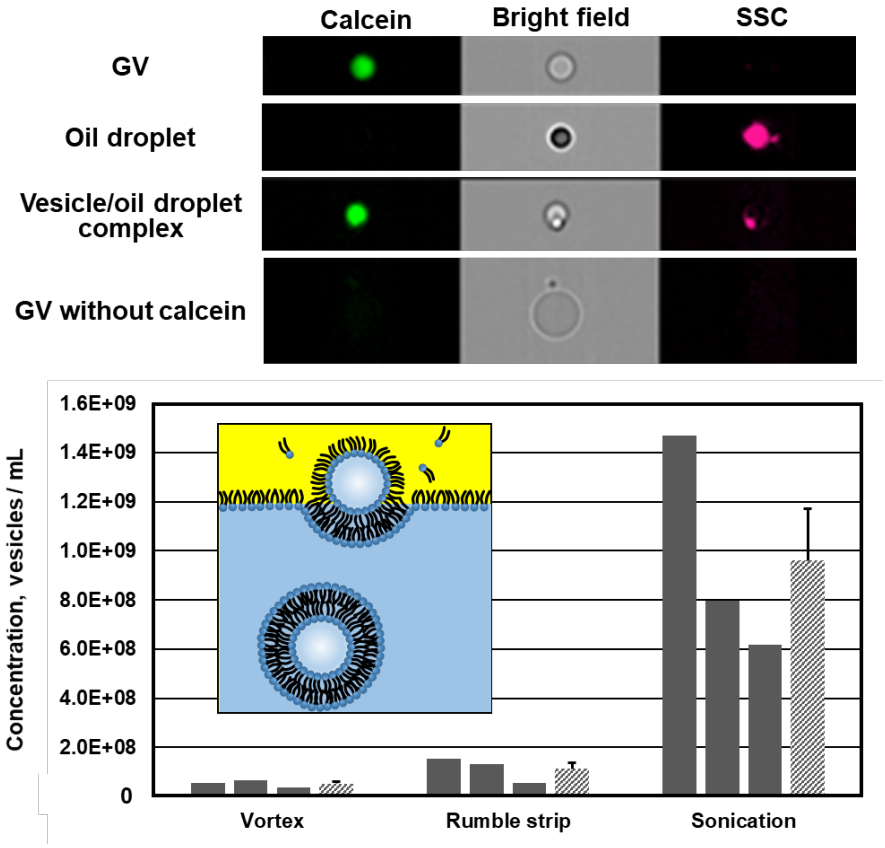

INTRODUCTION

Giant vesicles (GVs) are useful for studying the biochemical and biophysical properties of membranes and as model systems for living cells.[1-3] Due to their physical and functional mimicry of the cell membrane, GVs have also been used for researching lipid dynamics and membrane fusion.[4-6] Considering the complexity and long evolutionary history of living cells, an increasingly popular research objective is to drastically reduce the confounding nature of cells by constructing simple artificial vesicles and artificial cells. GVs consisting of phospholipid membranes, which can incorporate membrane proteins and encapsulate a minimal set of molecular components and biological reactions, are examples of such approaches. For example, there have been a number of recent reports about the activity assays of membrane proteins inserted into GVs.[2] The surrounding environment of membrane proteins is mimicked by specifying the lipid bilayer composition of GVs. Moreover, owing to their large size, functionalization of single vesicles can be observed by optical microscopy and the essential functions of membrane proteins can be revealed. GVs have also been used to understand cellular functions and diseases coupled to cytoskeletal dynamics with several studies focusing on the function of actin in GVs.[1,7] These reports demonstrated that actin filaments in GVs drastically change membrane dynamics and mechanics.[8-10] Another application using GVs

is to reconstitute the fundamental basis of living cells *in vitro*.[11] Such bottom-up approaches in synthetic biology may provide not only novel insights into a necessary and sufficient setting to construct biological systems but also a foundation for the development of new and innovative technologies.[12,13] Such an approach is also used to explore the transition from nonliving to living matter and to provide insight into the origin of life.

Various methods for preparing of GVs are well established.[3,14] Lipid hydration, electroformation, and the water-in-oil (w/o) emulsion transfer method have been reported as the most widely used methods for preparation of GVs. The lipid hydration method, which is based on simple principles relying on the hydration or swelling of a thin dry film of amphiphilic lipids, is the most common technique for preparing GVs because a neither a high degree of experimental sophistication nor special equipment are required.[15-17] However, it well known that it is difficult to control the experimental conditions of hydration or swelling for GV formation, resulting in the production of polydisperse vesicles as well as heterogeneous nested and multilamellar structures. Electroformation improved the production of GVs by enhancing the electrostatic repulsion between bilayer membranes with electric fields, although special equipment comprising of an observation chamber with electrodes and a power supply is required for the method.[18] Such methods

still lack the ability to efficiently encapsulate large quantities of water soluble molecules such as enzymes[19-22]. In comparison to lipid hydration and electroformation methods, the recently developed w/o emulsion transfer method has the advantage that encapsulation efficiency is markedly higher than other methods.[23,24] Another advantage is the fact that vesicles obtained by the w/o emulsion transfer methods are mainly unilamellar.[25,26] Therefore, the w/o emulsion transfer method can be valuable for producing reaction compartments and for mimicking biological systems.

The properties of GVs, such as size, membrane lamellarity, and vesicle structure, have been characterized because of the importance of these parameters in the above-mentioned studies. It is usually reported that these methods produce a population of GVs that are heterogeneous in structure. Most of the characterization has long been carried out by fluorescence microscopy using membrane associated dyes and water-soluble dyes as internal volume markers. However, this method has limits as to how quantitative the measurements can be, and it is difficult to acquire statistical population-level data and detect rare objects. Most recently, flow cytometry has been used to detect not only a wide variety of GVs but also biochemical reactions inside vesicles. The authors have also demonstrated quantitative analysis of structural properties of GVs.[27-30] However, any optical information has to be acquired independently of the flow cytometry data.[27]

Here we describe the preparation of GVs by the optimized w/o emulsion transfer method, and the quantitative and qualitative study of GVs by *imaging* flow cytometric analysis carried out on Amnis ImageStream Mark II. The imaging flow cytometer combines microscopy with traditional flow cytometry. Oil droplets, vesicles encapsulating oil droplets, and vesicles without intended content, were identified as byproducts. In addition, we have successfully quantified these products along with the desired GVs. Our quantitative analysis indicates that the production yield of GVs depends highly on the emulsification technique. Samples with sonication-based agitation exhibited significantly higher efficiencies of GV-production than that of vortex- and rumble strip-based methods. We recommend that using a sonication-based w/o emulsion transfer method and *imaging* flow cytometry on its products will be the most efficient means of producing and characterizing bespoke vesicles without including confounding byproducts in the analyses.

EXPERIMENTAL SECTION

Materials. 1-Palmitoyl-2-oleoyl-*sn*-glycero-3-phosphocholine (POPC) was purchased from Corder Pharma (Germany) and used without further purification. 0.1 mg/μL POPC stock solutions were prepared by directly dissolving the lipid in chloroform. Mineral oil (light oil, 0.840 g/mL) was purchased from Adamas-beta reagent (Shanghai, China). Calcein was purchased from Solarbio (Beijing, China). N-(2-hydroxyethyl) piperazine-N'-2-ethanesulfonic acid (HEPES), sucrose, and glucose were purchased from VETEC (China). Chloroform was purchased from Shanghai Richjoint Chemical Reagents (Shanghai, China). KOH was purchased from Sinopharm Chemical Reagent (Shanghai, China).

Preparation of GVs Encapsulating Calcein. GVs were prepared using the w/o emulsion transfer method with modifications to the protocol reported previously.[25] Two aqueous solutions were prepared: the inner aqueous solution [50 mM HEPES-KOH (pH 7.6), 500 mM sucrose, 2 mM calcein] and the bottom aqueous solution [50 mM HEPES-KOH (pH 7.6), 500 mM glucose]. The POPC stock solution was mixed with mineral oil to produce a 0.1 mg/mL POPC solution (lipid-carrying oil) and heated at 80˚C for 30 min in an open tube to completely dissolve the lipids and evaporate the chloroform. For

making w/o emulsion, 50 μL of inner aqueous solution and 400 μL of lipid-carrying oil were put into 2 mL microcentrifuge tube, and agitated either by vortexing (SCILOGEX, MX-S) for 40 sec, by dragging 50 times on microtube rack (now named rumble strip-based method), or by sonication using ultrasonic processor (SONICS & MATERIALS, INC, VCX750) on ice for 1 min, and equilibrated on ice for 10 min. 200 μL of the bottom aqueous solution was placed in a new microcentrifuge tube and w/o emulsion obtained in the step 3 was gently poured on top of the bottom aqueous solution. The tube was placed into the centrifuge (SIGMA, 1-14), left to stand for 5-10 mins to equilibrate the interface, and centrifuged at 16,100 x g for 15 min at room temperature. This produced a pellet of vesicles. The oil and the top of the aqueous phase were removed by aspiration and the pellet was gently resuspended by pipetting up and down. The suspension was collected from the bottom of tube and transferred into a new 600 μL microcentrifuge tube. As a washing step, 300 μL of extra bottom aqueous solution was added into the 600 μL tube and mixed with the suspension by pipetting up and down. The suspension was then centrifuged at 16,100 x g for 5 min at room temperature. The supernatant was removed by leaving 100 μL of the bottom solution and the sediment was gently resuspended for storage or directly used for analysis.

Imaging Flow Cytometry Analysis. The fluorescence intensities from encapsulated calcein in individual GVs were measured by using the imaging flow cytometer ImageStream Mark II and INSPIRE acquisition software (Amnis/Millipore). We obtained 50,000 data points for each measurement and analyzed the data by IDEAS analysis software (Amnis/Millipore). Calcein was excited with a 488 nm laser and the emission was detected with 505–560 nm filter in Channel 2, bright field data was collected in Channel 4, and side scatter (SSC) data was collected in Channel 6 at a 785 nm. All samples were acquired with 40x magnification, providing a pixel size of 0.25 μm^2, and with low flow rate/high sensitivity. In this type of flow cytometry, internal size standard beads are run concurrently and used for daily calibration as well as for the real-time velocity detection and autofocusing. Analysis of GVs was performed according to Figure S1.

RESULTS AND DISCUSSION

Establishment of the Method for Analyzing GVs Encapsulating Calcein by Imaging Flow Cytometry. The GVs encapsulating calcein were prepared by a modified w/o emulsion transfer method as described above.[25] The first step is the formation of a stable w/o emulsion by dispersion of the inner aqueous solution in mineral oil containing POPC (Figure 1A). Calcein was added to the inner aqueous phase enabling quantitative analysis of GVs by flow cytometry. To provide a difference in specific gravity between the inner aqueous phase and outer aqueous phase while maintaining equal pH and osmolarity across the membrane, we used HEPES buffer containing 500 mM sucrose as the inner aqueous solution and HEPES buffer containing 500 mM glucose as the bottom aqueous solution (Figure 1B). It should be noted that the w/o emulsion phase contains free lipids which form a lipid monolayer at the oil-water interface. GVs are formed when the water droplets pass through the oil-water interface and acquire an additional lipid monolayer. After removing the upper oil phase by aspiration (Figure 1C), a solution of vesicles remains. We used the imaging flow cytometer, ImageStream^X Mark II, to characterize the GVs as described in the Materials and Methods. Every sample used to establish the analysis methods for *imaging* flow cytometry was created using the vortex-based w/o emulsion transfer method.

Populations of Vesicle Products by W/O Emulsion Transfer Method. First, we attempted to identify the populations of vesicle products by *imaging* flow cytometry. It has been reported that oil droplets and lipid aggregates/complexes with oil inclusions are produced as byproducts of the w/o emulsion transfer method.[31-33] We found a population that has higher SSC intensity and a larger size than the calibration beads in the plots of SSC intensity versus bright field area, and gated it as Unknown-1 region (Figure 2, left side panel). Green fluorescence was not detected in the Unknown-1 population, indicating that they do not encapsulate the aqueous volume marker calcein (Figure 2, left side panel). A population deviating from the main curve that has calcein fluorescence and partial SSC signal was also found and labelled as Unknown-2a/b/c in the plots of SSC intensity versus bright field area (Figure 2, right side panel). It should be noted that GVs encapsulating calcein have an extremely weak SSC signal. To examine whether either Unknown-1 or 2 is derived from oil droplets, we prepared oil-in-water (o/w) emulsions and analyzed them (see Supporting Information and Figure S2). The o/w emulsion droplets were detected in Unknown-1 region, and the qualitative features of bright field and SSC were similar to those found for prepared GVs (Figure 2, left side panel). These data suggest that oil droplets were the main component of Unknown-1 population. We

hypothesize that it is likely that the Unknown-2 population is derived from GVs encapsulating oil droplets or lipid aggregates/complexes (Figure 2, right side panel). We plotted the SSC intensity versus calcein fluorescence intensity (Figure 3, left side panel, in which Unknown-1s are shown as blue dots and Unknown-2s are shown as pink dots) and found that the Unknown-2 population has characteristics lying between that of oil droplets (Unknown-1) and GVs, consistent with our hypothesis. If it is assumed that Unknown-1 population is derived from oil droplets, the Unknown-1 population should be decreased by eliminating the oil droplets. To examine this hypothesis, we attempted to remove the oil droplets by spontaneous precipitation of original GVs prepared by the vortex-based method (see Supporting Information). Indeed, the Unknown-1 content detected in Figure 3 (blue dots in left side panel) was decreased after spontaneous precipitation (Figure S3, Unknown-1 contents in the sample for before and after spontaneous precipitation were 0.69% and 0.13%, respectively). These data indicate that a small amount of oil droplets also sediment with GVs by centrifugation or adhere to the microcentrifuge tube and resist buoyancy. To further verify the populations, we created a scatter diagram where the calcein fluorescence intensity is plotted versus bright field area (Figure 4, middle panel). The logarithm of the bright field area scales linearly with the logarithm of calcein fluorescence intensity for most of the data points with a

subpopulation deviating from the line (black gate in Figure 4). As clearly shown in Figure 4, this population includes objects that have no calcein fluorescence (Figure 4, right side panel). It is possible that this population contains the bottom aqueous solution; in other words, partially ruptured GVs may reform GVs in the bottom aqueous phase as suggested previously.[31] Together, these data suggest that products obtained by w/o emulsion transfer method contain small percentages of different kinds of byproducts, such as oil droplets, vesicles encapsulating oil droplets, and vesicles containing no internal aqueous marker.

Furthermore, we found that GVs prepared by the vortex-based w/o emulsion transfer method have a mean diameter of 4.1 μm when considering only single vesicles (Supporting Information and Figure S1), agreeing with previous reports of POPC GVs having mean diameters of around 10 μm.[25,34]

Comparing Three Different Emulsification Techniques. We examined the efficiencies in producing GVs of three methods; vortex-, rumble strip-, and sonication-based w/o emulsion transfer method as described in Materials and Methods. A summary of the results is shown in Table 1.

First, we compared the yields to assess the efficiencies of three techniques in producing GVs. Since ImageStream^X Mark II uses syringe pumps, which can be

converted to the consumed volume for data acquisition, the injected sample volume with particle counts can be used to calculate the particle concentration with high accuracy. As shown in Figure 5A and Table 1, GVs were obtained in higher yield (9.60×10^8 vesicles/mL) in the sonication-based w/o emulsion transfer method than in the vortex- and the rumble strip-based methods (5.27×10^7 vesicles/mL and 1.13×10^8 vesicles/mL, respectively). Our results agree with previous reports that one of advantages of the w/o emulsion transfer method is the fact this method can achieve high production yields.[3,14] Furthermore, our results suggest that production yield of GV depends on the emulsification technique. In the emulsions created by vortex- and the rumble strip-based agitation, sedimentation of w/o droplets containing fluorescent dye under gravity was observed owing to their insufficient dispersion, whereas emulsions prepared by sonication appear to have a good temporal dispersion (Figure 5B). Further, breakdown of w/o droplets happened when the w/o emulsion was gently poured on top of the bottom aqueous solution (Figure 1B); fluorescence was observed in lower layer for vortexed and rumble strip-agitated emulsions but not for sonicated emulsions (Figure 5C). We conclude that vortexing and rumble strip agitation may not provide enough kinetic energy to yield small enough droplets that are stable to sedimentation.

We next examined the purity of GVs prepared by the three methods. SSC intensity versus calcein fluorescence intensity plots for each methods can help distinguish between the different products and is shown in Figure 6A-C. The vortex-based method yields a slightly higher (~2%) population of both oil droplets and lipid complexes/aggregates compared to the other two methods (see also Table 1). We also noticed that the signals of Predicted to be GVs (Figure 6A, black dots) were broadly distributed and rather close to Unknown-2 (Figure 6A, pink dots) for the vortex-based method, while a clearer separation between the regions was found for the rumble strip-based and the sonication-based methods owing to the narrower distribution of particles predicted to be GVs (Figure 6B and C). These data suggest that cleaner GVs, which are free of oil droplet inclusions, can be obtained by the rumble strip-based and sonication-based methods. Final purities of GVs in each method were also calculated by using the plots of the calcein fluorescence intensity versus bright field area (Figure 6D-F, Table 1) with the vortex-based method having a slightly decreased purity compared to the rumble strip- and the sonication-based methods. In any case, these data indicate that particles prepared by the w/o emulsion transfer method, for all three emulsification techniques, was greater than 90% GVs as judged from imaging flow cytometric analysis.

Interestingly, most w/o droplets prepared by our emulsification methods have a particle diameter less than 4 μm whereas the produced GVs have a wider size distribution, with the mean diameter being greater than 4 μm (Figure S4). We hypothesize that the coalescence of w/o droplets occurs before or during the transfer step although little is known about the mechanisms involved. Future studies will be required to reveal the detailed mechanisms of the w/o emulsion transfer method. We also found that GVs prepared by the sonication-based w/o emulsion transfer method have slightly larger sizes (a mean particle diameter of 4.5 μm) than the GVs obtained by the vortex- (4.1 μm) and the rumble strip-based methods (3.9 μm) (Table 1). It has been reported that competition between gravitational and bending energies also determines the transportation behavior.[35] From this report, the theoretically calculated transition size of vesicle is in the micro-meter range when using 1 M and 100 mM sugar solutions for w/o emulsion transfer methods, in agreement with our results. Taken together, our data suggest that the sonication-based emulsion method provide a w/o droplet size suitable for the formation of stable GVs in our experimental system.

CONCLUSIONS

Here we present a protocol for analyzing GVs prepared by the w/o emulsion transfer method with *imaging* flow cytometry. Through image-based analyses, the populations of vesicle products were identified. The products obtained by the w/o emulsion transfer method contain, in addition to GVs, oil droplets, vesicle/oil droplet complexes, and vesicles encapsulating no aqueous volume marker. The mean of GV size (>4 μm diameter) was determined optically. Thus, we have demonstrated that both quantitative and qualitative analysis by *imaging* flow cytometry can enhance our understanding of properties of GVs prepared by the w/o emulsion transfer method. In addition, we validated three different emulsification methods and demonstrated that sonication-based agitation exhibits the highest efficiency in producing GVs (~10 times higher than that of vortex- and rumble strip-based methods). We anticipate that using a sonication-based w/o emulsion transfer method and *imaging* flow cytometric analysis on its products will be useful for further development of GV research towards artificial membrane and artificial cells research.

AUTHOR INFORMATION

Corresponding Author

*E-mail: yomo@sei.ecnu.edu.cn, tetsuyayomo@gmail.com

ORCID

Tetsuya Yomo: 0000-0003-3116-107X

Funding

This work was supported by MOE International Joint Lab of Trustworthy Software at East China Normal University. A.W. is supported by the NASA postdoctoral Program. J.W.S is an investigator of the Howard Hughes Medical Institute. This work was supported in part by a grant (290363) from the Simons Foundation to J.W.S.

Notes

The authors declare no competing financial interest.

References

(1) Fenz, S. F.; Sengupta, K. Giant vesicles as cell models. *Integrative biology : quantitative biosciences from nano to macro* **2012**, *4*, 982-995.

(2) Jorgensen, I. L.; Kemmer, G. C.; Pomorski, T. G. Membrane protein reconstitution into giant unilamellar vesicles: a review on current techniques. *European biophysics journal : EBJ* **2017**, *46*, 103-119.

(3) Walde, P.; Cosentino, K.; Engel, H.; Stano, P. Giant vesicles: preparations and applications. *Chembiochem : a European journal of chemical biology* **2010**, *11*, 848-865.

(4) Chernomordik, L. V.; Kozlov, M. M. Mechanics of membrane fusion. *Nature structural & molecular biology* **2008**, *15*, 675-683.

(5) Marsden, H. R.; Tomatsu, I.; Kros, A. Model systems for membrane fusion. *Chemical Society reviews* **2011**, *40*, 1572-1585.

(6) Beales, P. A.; Ciani, B.; Cleasby, A. J. Nature's lessons in design: nanomachines to scaffold, remodel and shape membrane compartments. *Phys Chem Chem Phys* **2015**, *17*, 15489-15507.

(7) Bruggemann, D.; Frohnmayer, J. P.; Spatz, J. P. Model systems for studying cell adhesion and biomimetic actin networks. *Beilstein journal of nanotechnology* **2014**, *5*,

1193-1202.

(8) Guevorkian, K.; Manzi, J.; Pontani, L. L.; Brochard-Wyart, F.; Sykes, C. Mechanics of Biomimetic Liposomes Encapsulating an Actin Shell. *Biophysical journal* **2015**, *109*, 2471-2479.

(9) Takiguchi, K.; Yamada, A.; Negishi, M.; Tanaka-Takiguchi, Y.; Yoshikawa, K. Entrapping desired amounts of actin filaments and molecular motor proteins in giant liposomes. *Langmuir : the ACS journal of surfaces and colloids* **2008**, *24*, 11323-11326.

(10) Tanaka, S.; Takiguchi, K.; Hayashi, M. Repetitive stretching of giant liposomes utilizing the nematic alignment of confined actin. *Commun Phys* **2018**, *1*.

(11) Gopfrich, K.; Platzman, I.; Spatz, J. P. Mastering Complexity: Towards Bottom-up Construction of Multifunctional Eukaryotic Synthetic Cells. *Trends in biotechnology* **2018**.

(12) Hanczyc, M. M.; Fujikawa, S. M.; Szostak, J. W. Experimental models of primitive cellular compartments: encapsulation, growth, and division. *Science* **2003**, *302*, 618-622.

(13) Chen, I. A.; Roberts, R. W.; Szostak, J. W. The emergence of competition between model protocells. *Science* **2004**, *305*, 1474-1476.

(14) Jimenez, M.; Martos, A.; Cabre, E. J.; Raso, A.; Rivas, G. Giant vesicles: a powerful tool to reconstruct bacterial division assemblies in cell-like compartments. *Environmental microbiology* **2013**, *15*, 3158-3168.

(15) Reeves, J. P.; Dowben, R. M. Formation and properties of thin-walled phospholipid vesicles. *Journal of cellular physiology* **1969**, *73*, 49-60.

(16) Tsumoto, K.; Matsuo, H.; Tomita, M.; Yoshimura, T. Efficient formation of giant liposomes through the gentle hydration of phosphatidylcholine films doped with sugar. *Colloids and surfaces. B, Biointerfaces* **2009**, *68*, 98-105.

(17) Ishikawa, K.; Sato, K.; Shima, Y.; Urabe, I.; Yomo, T. Expression of a cascading genetic network within liposomes. *FEBS letters* **2004**, *576*, 387-390.

(18) Bothorel, M. I. A. S. M. F. Preparation of giant vesicles by external AC electric fields. Kinetics and applications. *Progress in Colloid & Polymer Science* **1992**, *89*, 127-131.

(19) Luisi, P. L.; Allegretti, M.; Pereira de Souza, T.; Steiniger, F.; Fahr, A.; Stano, P. Spontaneous protein crowding in liposomes: a new vista for the origin of cellular metabolism. *Chembiochem : a European journal of chemical biology* **2010**, *11*, 1989-1992.

(20) de Souza, T. P.; Steiniger, F.; Stano, P.; Fahr, A.; Luisi, P. L. Spontaneous Crowding

of Ribosomes and Proteins inside Vesicles: A Possible Mechanism for the Origin of Cell Metabolism. *Chembiochem : a European journal of chemical biology* **2011**, *12*, 2325-2330.

(21) Stano, P.; de Souza, T. P.; Carrara, P.; Altamura, E.; D'Aguanno, E.; Caputo, M.; Luisi, P. L.; Mavelli, F. Recent Biophysical Issues About the Preparation of Solute-Filled Lipid Vesicles. *Mech Adv Mater Struc* **2015**, *22*, 748-759.

(22) Stano, P.; D'Aguanno, E.; Bolz, J.; Fahr, A.; Luisi, P. L. A remarkable self-organization process as the origin of primitive functional cells. *Angewandte Chemie* **2013**, *52*, 13397-13400.

(23) Pautot, S.; Frisken, B. J.; Weitz, D. A. Production of unilamellar vesicles using an inverted emulsion. *Langmuir : the ACS journal of surfaces and colloids* **2003**, *19*, 2870-2879.

(24) Pautot, S.; Frisken, B. J.; Weitz, D. A. Engineering asymmetric vesicles. *Proceedings of the National Academy of Sciences of the United States of America* **2003**, *100*, 10718-10721.

(25) Nishimura, K.; Hosoi, T.; Sunami, T.; Toyota, T.; Fujinami, M.; Oguma, K.; Matsuura, T.; Suzuki, H.; Yomo, T. Population analysis of structural properties of giant liposomes by flow cytometry. *Langmuir : the ACS journal of surfaces and colloids*

2009, *25*, 10439-10443.

(26) Chiba, M.; Miyazaki, M.; Ishiwata, S. Quantitative analysis of the lamellarity of giant liposomes prepared by the inverted emulsion method. *Biophysical journal* **2014**, *107*, 346-354.

(27) Sato, K.; Obinata, K.; Sugawara, T.; Urabe, I.; Yomo, T. Quantification of structural properties of cell-sized individual liposomes by flow cytometry. *Journal of bioscience and bioengineering* **2006**, *102*, 171-178.

(28) Hosoda, K.; Sunami, T.; Kazuta, Y.; Matsuura, T.; Suzuki, H.; Yomo, T. Quantitative study of the structure of multilamellar giant liposomes as a container of protein synthesis reaction. *Langmuir : the ACS journal of surfaces and colloids* **2008**, *24*, 13540-13548.

(29) Sunami, T.; Caschera, F.; Morita, Y.; Toyota, T.; Nishimura, K.; Matsuura, T.; Suzuki, H.; Hanczyc, M. M.; Yomo, T. Detection of association and fusion of giant vesicles using a fluorescence-activated cell sorter. *Langmuir : the ACS journal of surfaces and colloids* **2010**, *26*, 15098-15103.

(30) Nishimura, K.; Suzuki, H.; Toyota, T.; Yomo, T. Size control of giant unilamellar vesicles prepared from inverted emulsion droplets. *Journal of colloid and interface science* **2012**, *376*, 119-125.

(31) Whittenton, J.; Harendra, S.; Pitchumani, R.; Mohanty, K.; Vipulanandan, C.; Thevananther, S. Evaluation of asymmetric liposomal nanoparticles for encapsulation of polynucleotides. *Langmuir : the ACS journal of surfaces and colloids* **2008**, *24*, 8533-8540.

(32) Kubatta, E. A.; Rehage, H. Characterization of giant vesicles formed by phase transfer processes. *Colloid Polym Sci* **2009**, *287*, 1117-1122.

(33) Yamada, A.; Yamanaka, T.; Hamada, T.; Hase, M.; Yoshikawa, K.; Baigl, D. Spontaneous transfer of phospholipid-coated oil-in-oil and water-in-oil micro-droplets through an oil/water interface. *Langmuir : the ACS journal of surfaces and colloids* **2006**, *22*, 9824-9828.

(34) Tsuji, G.; Fujii, S.; Sunami, T.; Yomo, T. Sustainable proliferation of liposomes compatible with inner RNA replication. *Proceedings of the National Academy of Sciences of the United States of America* **2016**, *113*, 590-595.

(35) Hamada, T.; Miura, Y.; Komatsu, Y.; Kishimoto, Y.; Vestergaard, M.; Takagi, M. Construction of asymmetric cell-sized lipid vesicles from lipid-coated water-in-oil microdroplets. *The journal of physical chemistry. B* **2008**, *112*, 14678-14681.

Figures legends

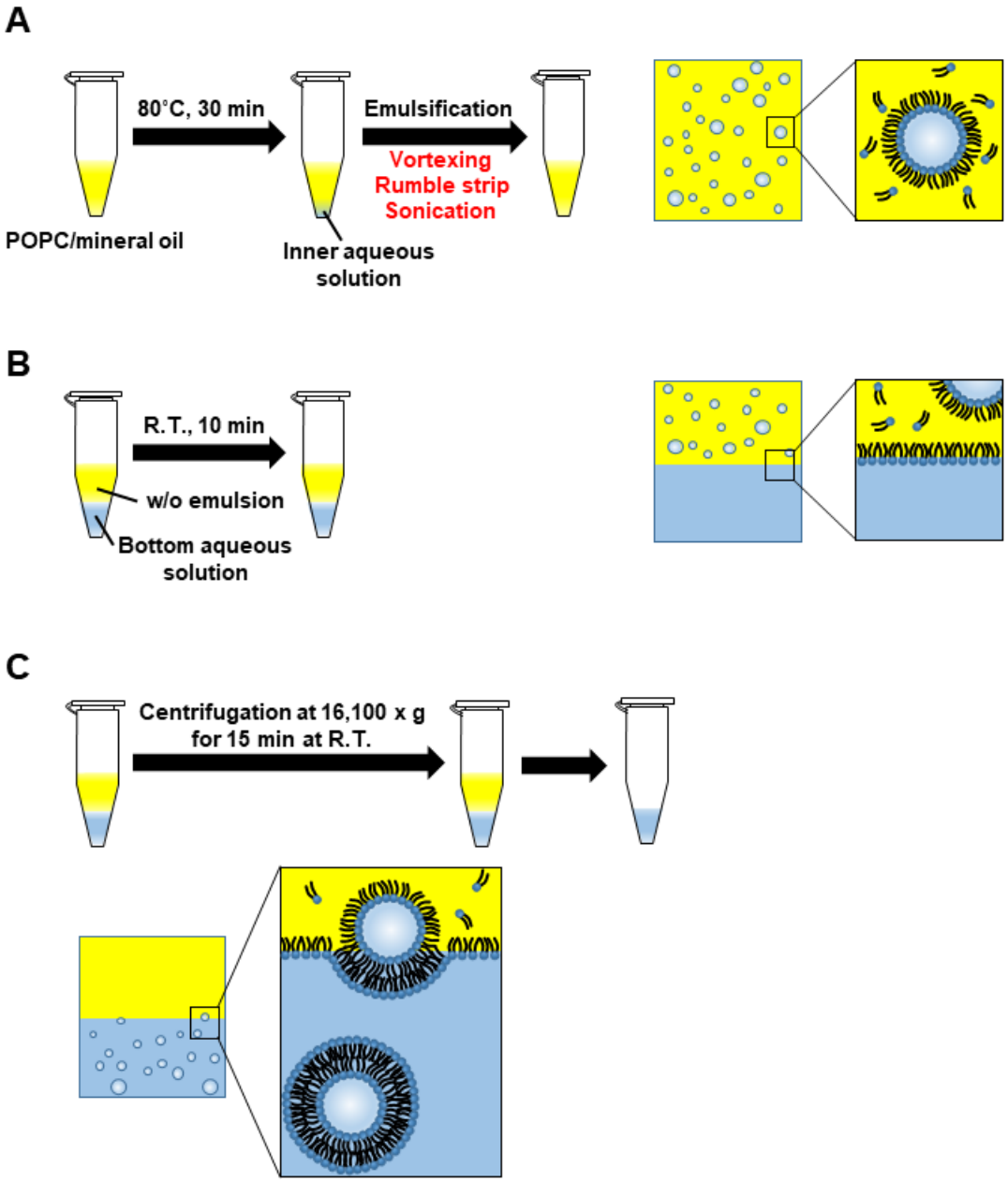

Figure 1. Schematic illustration of the w/o emulsion transfer methodology. (A) Formation of w/o emulsion using three different emulsification methods. The left side shows the macroscopic detail of the POPC/mineral oil mix (yellow) in the preparation tube. The

aqueous solution is shown as light blue. The right side panels illustrate the detail of the w/o emulsion. POPC, which is an amphiphilic phospholipid, is composed of a hydrophilic head (colored blue) and two hydrophobic tails (colored black). (B) Formation of a lipid monolayer at the oil-water interface. The right panels illustrate the detail of the oil-water interface. (C) Formation of GVs. The lower panels illustrate the GV formation process at the oil-water interface.

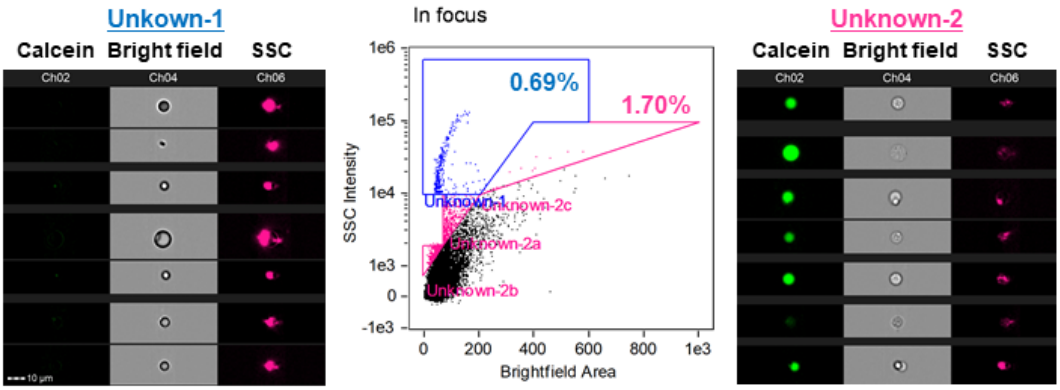

Figure 2. Identification of the populations of vesicle products. Scatter diagram of SSC intensity versus bright field area (middle panel). Blue gate denotes Unknown-1 and pink gates denote Unknown-2. Representative images of objects classified as Unknown-1 and as Unknown-2 are shown in the left side and the right side panel, respectively.

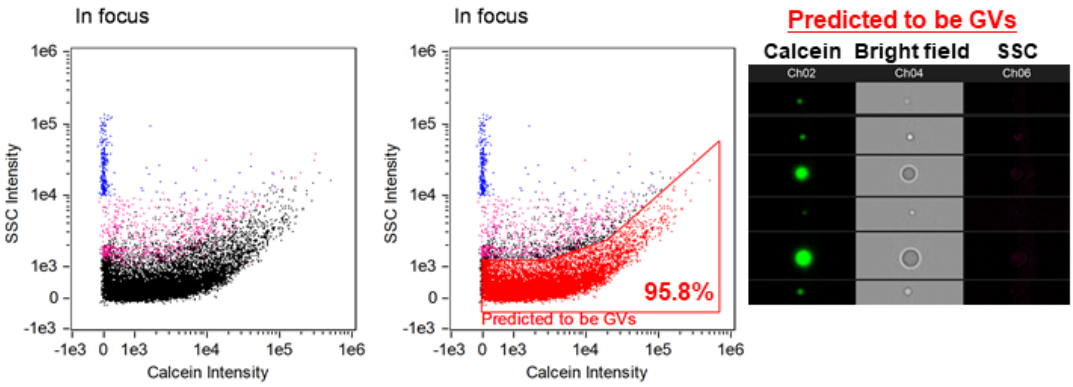

Figure 3. Scatter diagram of SSC intensity versus calcein fluorescence intensity (left side and middle panels). Unknown-1s and Unknown-2s are shown as blue dots and as pink dots, respectively. Red gate denotes Predicted to be GVs (middle panel). Representative images of objects classified as Predicted to be GVs is shown in the right side panel.

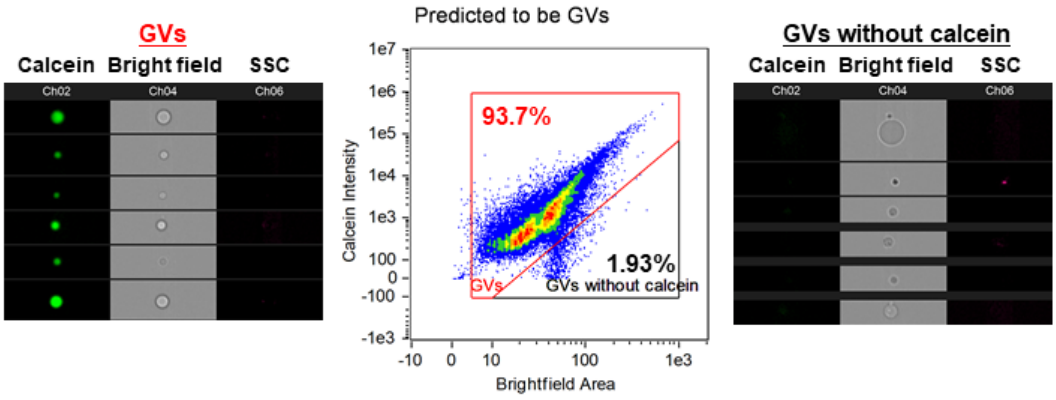

Figure 4. Scatter diagram of calcein fluorescence intensity versus bright field area. GVs and GVs without calcein were denoted as red gate and black gate, respectively. Representative images of objects classified as GVs and GVs without calcein are shown in the left side and the right side panel, respectively.

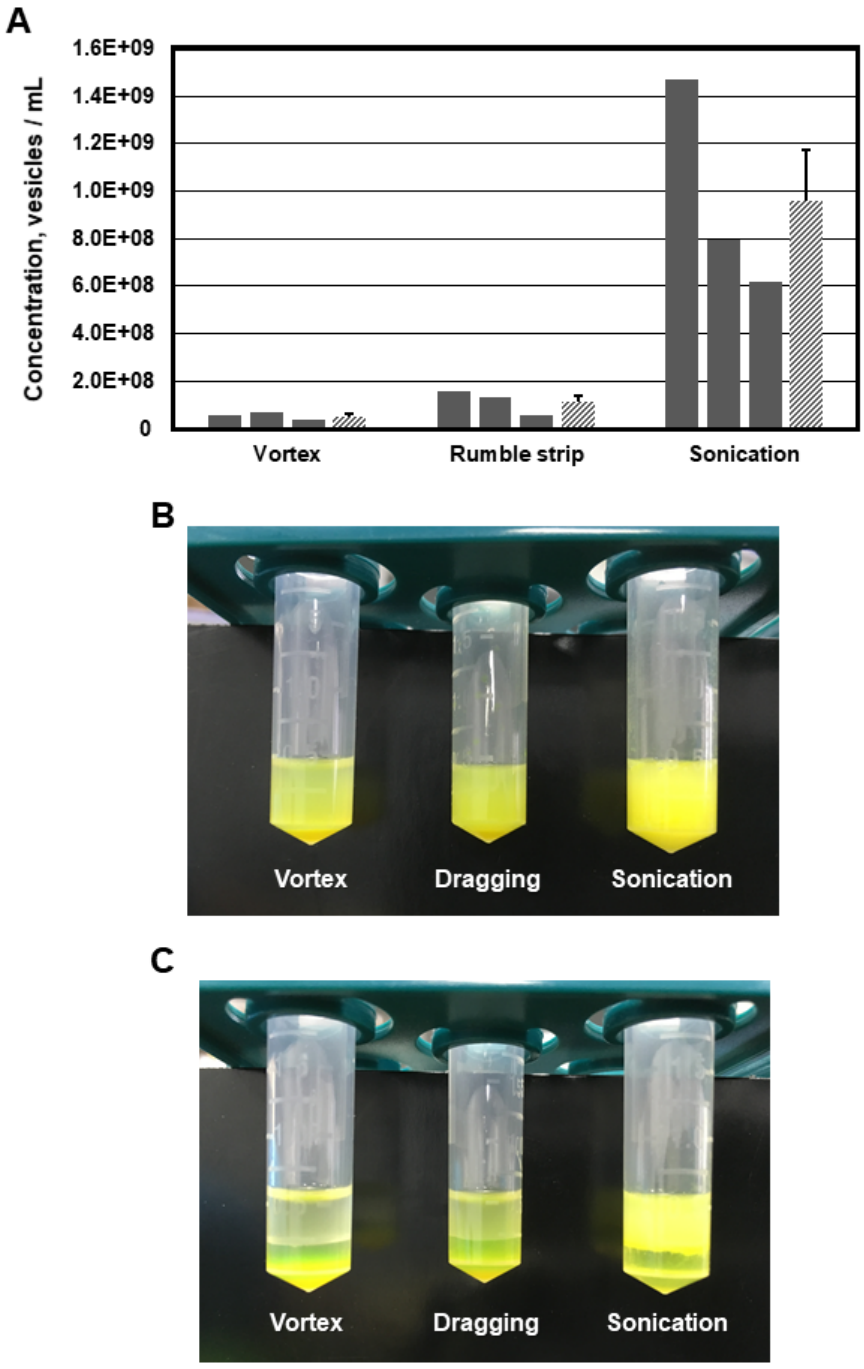

Figure 5. Comparison of the efficiency in producing GVs between the three methods. (A) GV concentration calculated by *imaging* flow cytometry in each method. GV concentration of each experiment (gray bars) and the mean of each method (diagonal

bars) are shown. Data represent the means ± SE, n = 3. (B) A photograph of the w/o emulsion prepared by three different emulsification techniques. The image shows the different distributions of the aqueous calcein as well as differences in turbidity. (C) A photograph of the step for the formation of a lipid monolayer at the oil-water interface by layering the POPC/mineral oil mix w/o emulsions on top of the bottom aqueous solution (see Figure 1B).

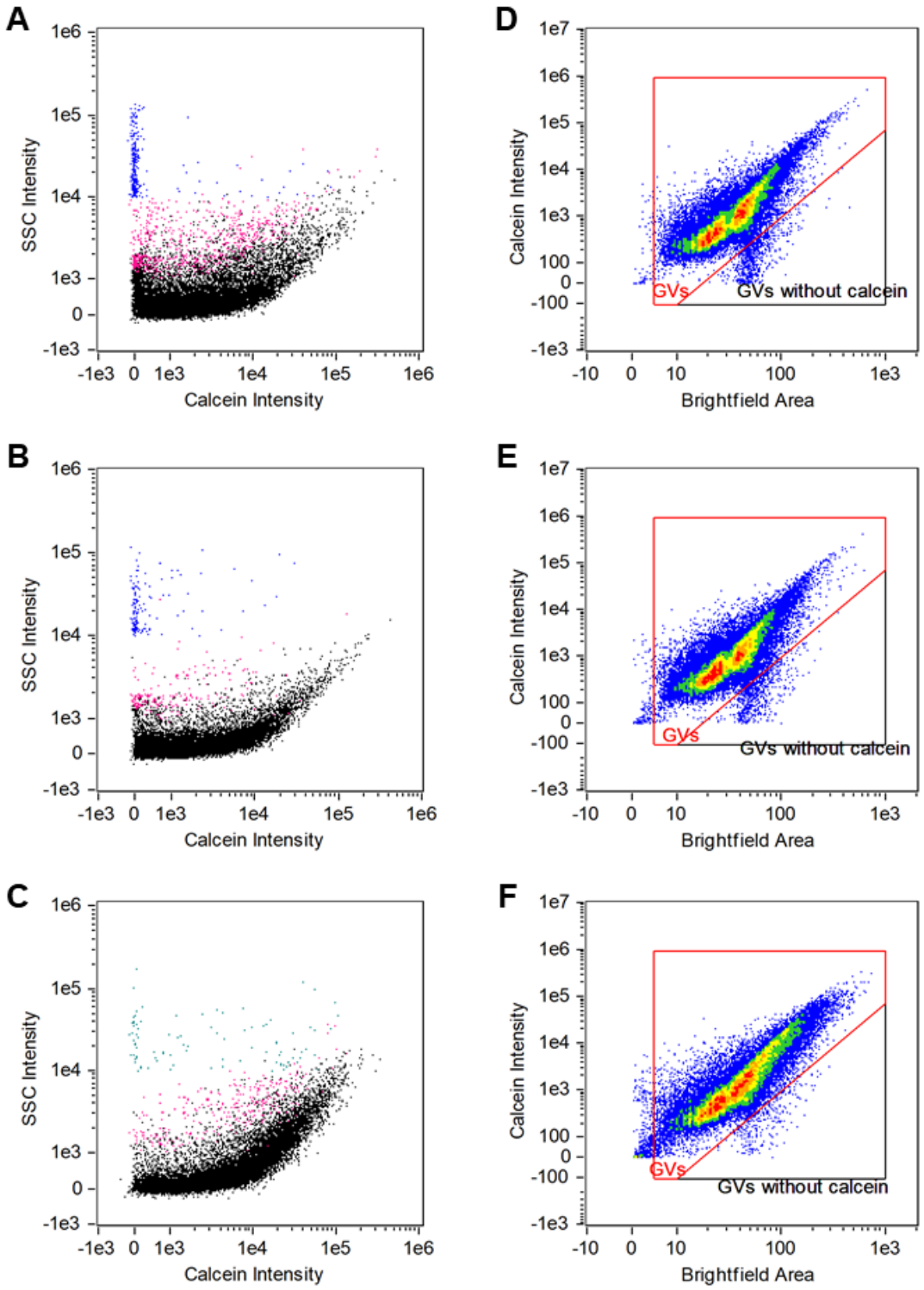

Figure 6. Comparison of the purity of GVs between the three methods. Scatter diagram of SSC intensity versus calcein fluorescence intensity for (A) vortex-based method, (B)

rumble strip-based method, and (C) sonication-based method, and scatter diagram of calcein fluorescence intensity versus bright field area for (D) vortex-based method, (E) rumble strip-based method, and (F) sonication-based method.

Table 1 Comparison between three emulsification techniques [a]

		Vortexing	Rumble strip	Sonication
Byproducts (%)	GVs without calcein	2.75	2.30	1.36
	Oil droplets (Unknown-1)	0.50	0.20	0.21
	GUVs encapsulating oil droplets (Unknown-2)	1.37	0.35	0.80
Final GV purity (%)		93.5	96.4	95.2
Vesicle diameter (micrometer)		4.1	3.9	4.5
Vesicle concentration (vesicles/mL)		5.27.E+07	1.13.E+08	9.60.E+08

[a] Data represent the means, n = 3.

Supporting Information for

Using Imaging Flow Cytometry to Quantify and Optimize Giant Vesicle Production by Water-in-oil Emulsion Transfer Methods

Yuka Matsushita-Ishiodori, Martin M. Hanczyc, Anna Wang, Jack W. Szostak, and Tetsuya Yomo*

Corresponding Author

*E-mail: yomo@sei.ecnu.edu.cn, tetsuyayomo@gmail.com

Page 5

Figures 4

Supporting Information Experimental Procedures (Materials and Methods)

-Preparation of o/w emulsion control. For making o/w emulsion, 400 μL of bottom aqueous solution and 50 μL of lipid-carrying oil were put into 2 mL centrifuge tube, and prepared by vortexing for 40 sec.

-Spontaneous precipitation. After preparing GVs by the vortex-based w/o emulsion transfer method, the tube containing the GVs was left in the dark for 2.5 h. 10 μL of sediment was collected from the bottom of tube and transferred into a new 600 μL tube. 10 μL of extra bottom aqueous solution was added into the 600 μL tube and mixed by pipetting up and down for storage or directly used for analysis.

Supporting Information Figures Legends

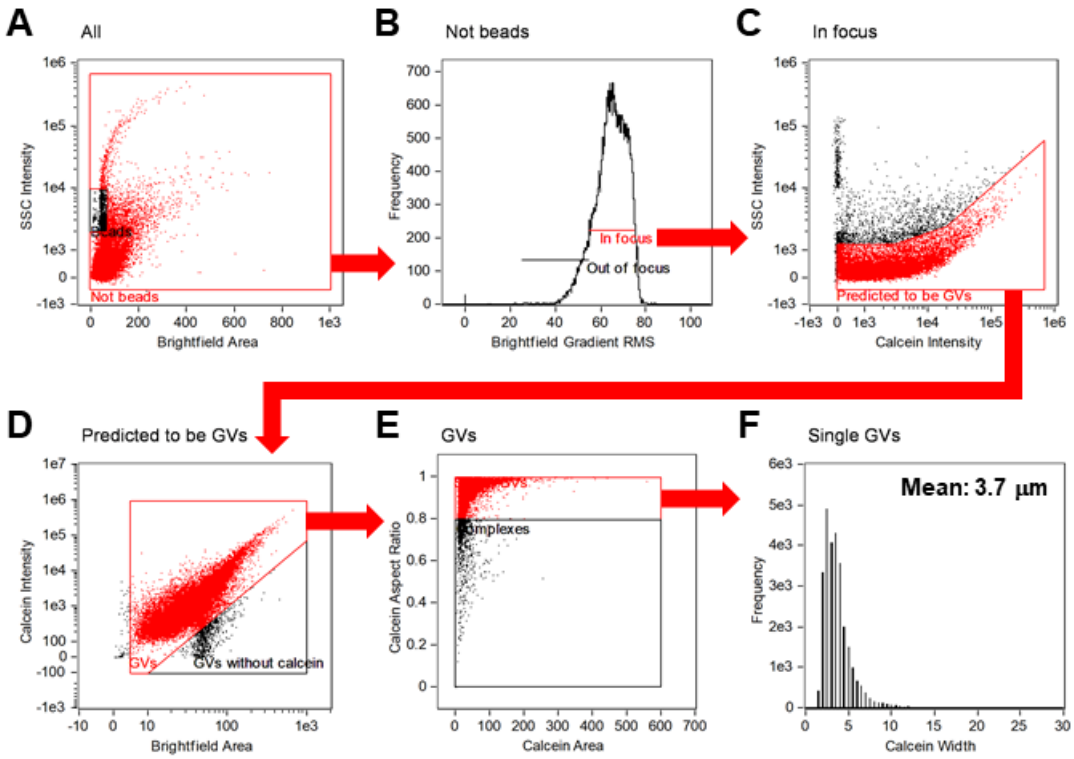

Figure S1. Overview of the sequential gating for flow cytometric analysis. (A) Separation of target objects from the internal calibration beads using a scatter diagram of SSC intensity versus bright field area. Target objects were selected as Not beads (red gate) and used in the next step. (B) Selection of the objects that are in focus using a histogram for bright field gradient RMS. In focus (red gate) were selected for the next step. (C) Discrimination of the objects predicted to be GVs from other byproducts, such as oil droplets, using a scatter diagram of SSC intensity versus calcein fluorescence intensity. The objects predicted to be GVs were denoted as red gate and used in the next step. (D) Discrimination of the object GVs from other byproducts that have no calcein fluorescence using a scatter diagram of calcein fluorescence intensity versus bright field area. GVs containing calcein (red gate) were selected for the next step. (E)

Discrimination of single GVs from doublets or fused vesicles using a scatter diagram of calcein fluorescence aspect ratio versus calcein fluorescence area. Single GVs (red gate) were selected for the next feature analysis. (F) Histogram for calcein fluorescence width correlated with the width of the GVs.

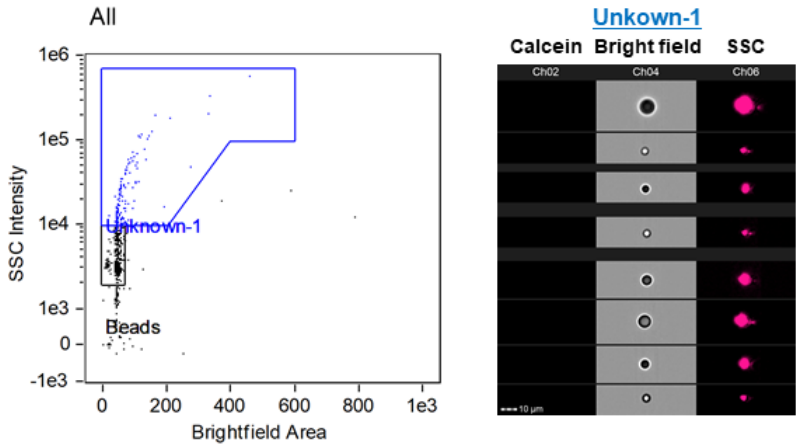

Figure S2. Scatter diagram of SSC intensity versus bright field area for the o/w emulsion. Representative images of objects in Unknown-1 region (blue gate) are shown in the right side panel.

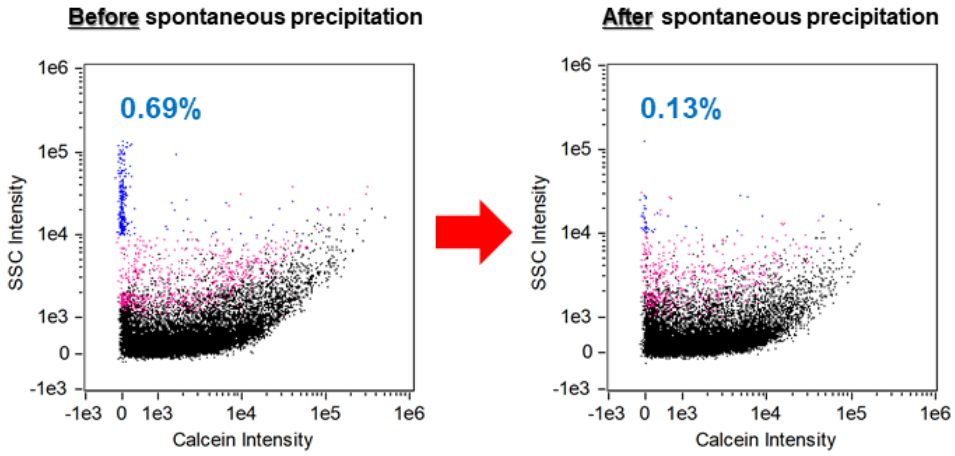

Figure S3. Scatter diagram of SSC intensity versus calcein fluorescence intensity for the samples before and after spontaneous precipitation. Unknown-1s and Unknown-2s are shown as blue dots and as pink dots, respectively.

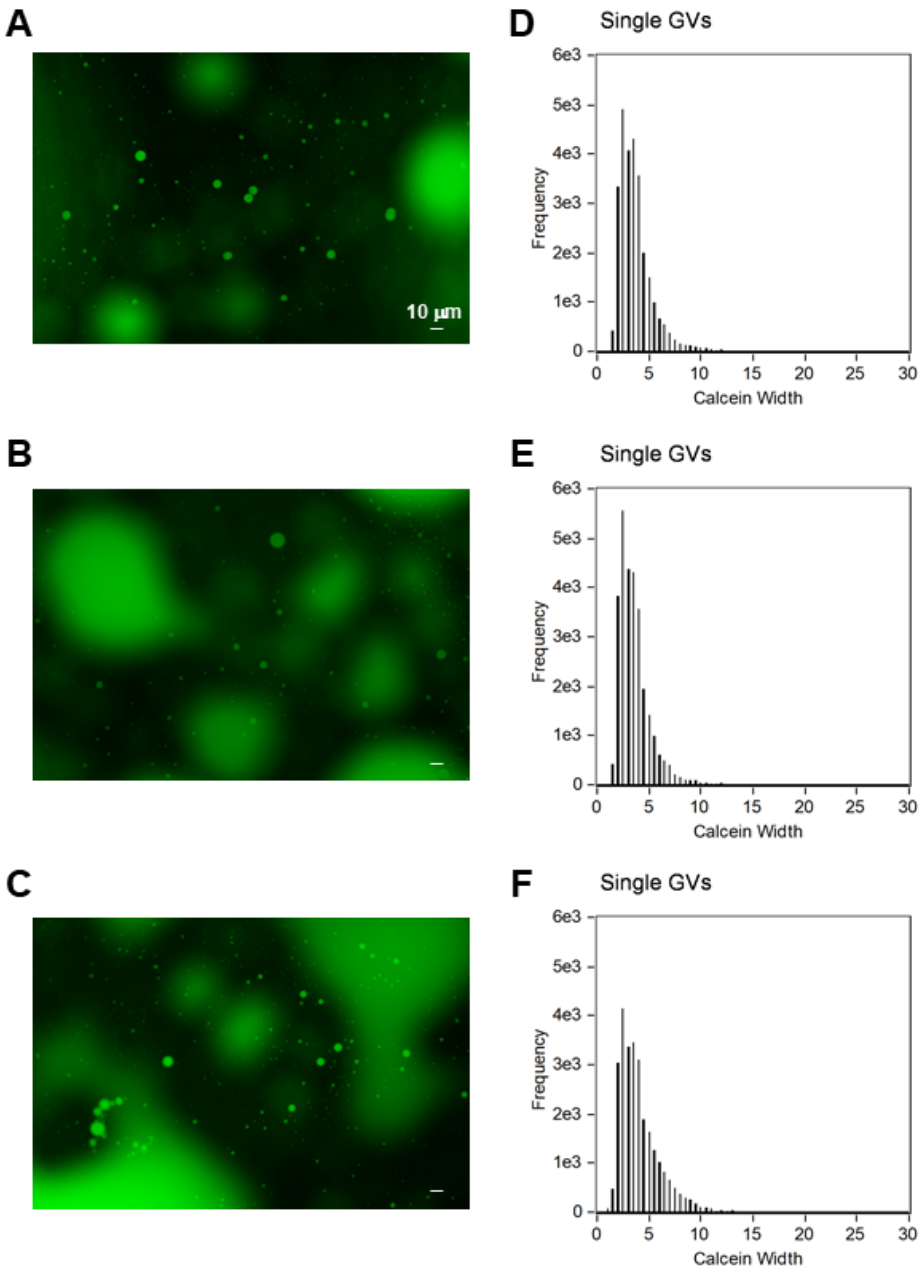

Figure S4. Comparison of the w/o emulsion droplets and GV sizes. Representative images of w/o emulsion droplets for (A) vortex-based method, (B) rumble strip-based method, and (C) sonication-based method, and histogram for calcein fluorescence width for (D) vortex-based method, (E) rumble strip-based method, and (F) sonication-based method.